Methods in Oceanography 17 (2016) 1–13

Contents lists available at ScienceDirect

Methods in Oceanography

journal homepage: www.elsevier.com/locate/mio

Full length article

A sensor package for mapping pH and oxygen from mobile platforms

Philip J. Bresnahan [a,*], Taylor Wirth [a], Todd R. Martz [a], Andreas J. Andersson [a], Tyler Cyronak [a], Sydney D'Angelo [a], James Pennise [b], W. Kendall Melville [a], Luc Lenain [a], Nicholas Statom [a]

[a] Scripps Institution of Oceanography, University of California, San Diego, 9500 Gilman Drive, La Jolla, CA 92093, USA

[b] Ocean Discovery Institute, 2211 Pacific Beach Drive, Suite A, San Diego, CA 92109, USA

GRAPHICAL ABSTRACT

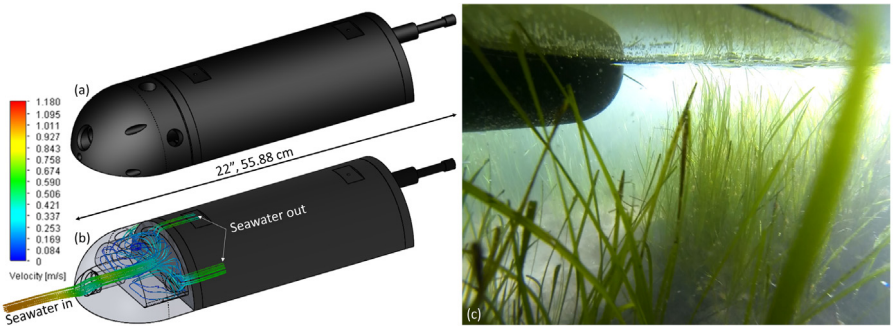

HIGHLIGHTS

- We designed a novel pH and oxygen sensor package specifically for mobile platforms.
- We mapped pH and dissolved oxygen in shallow, vegetated, hard-to-reach environments.
- The sensor performed very well (pH RMSE = 0.028) relative to discrete samples.
- 30 middle/high school students participated in supervised data collection/analysis.

* Correspondence to: San Francisco Estuary Institute, 4911 Central Ave, Richmond, CA 94804, USA.
E-mail address: philb@sfei.org (P.J. Bresnahan).

http://dx.doi.org/10.1016/j.mio.2016.04.004

ARTICLE INFO

Article history:
Received 10 January 2016
Received in revised form
7 April 2016
Accepted 27 April 2016
Available online 1 June 2016

Keywords:
pH
Oxygen
Sensor
Acidification
Mobile
Mapping

ABSTRACT

A novel chemical sensor package named "WavepHOx" was developed in order to facilitate measurement of surface ocean pH, dissolved oxygen, and temperature from mobile platforms. The system comprises a Honeywell Durafet pH sensor, Aanderaa optode oxygen sensor, and chloride ion selective electrode, packaged into a hydrodynamic, lightweight housing. The WavepHOx has been deployed on a stand-up paddleboard and a Liquid Robotics Wave Glider in multiple near-shore settings in the Southern California Bight. Integration of the WavepHOx into these mobile platforms has enabled high spatiotemporal resolution pH and dissolved oxygen data collection. It is a particularly valuable tool for mapping shallow, fragile, or densely vegetated ecosystems which cannot be easily accessed by other platforms. Results from three surveys in San Diego, California, are reported. We show pH and dissolved oxygen variability >0.3 and $>50\%$ saturation, respectively, over tens to hundreds of meters to highlight the degree of natural spatial variability in these vegetated ecosystems. When deployed during an extensive discrete sampling program, the WavepHOx pH had a root mean squared error of 0.028 relative to pH calculated from fifty six measurements of total alkalinity and dissolved inorganic carbon, confirming its capacity for accurate, high spatiotemporal resolution data collection.

1. Introduction

Coastal carbon budgets have proven particularly difficult to constrain due to their high levels of inter- and intra-ecosystem spatiotemporal heterogeneity (Borges, 2005; Borges et al., 2010, 2006; Chen and Borges, 2009; Gattuso et al., 1998; Laruelle et al., 2010). Current estimates suggest that continental shelves are a sink of 0.35 Pg C yr^{-1}, while inner estuaries, salt marshes, and mangroves forests are a source of 0.50 Pg C yr^{-1} (Cai, 2011). Nonetheless, uncertainty in continental shelf and coastal CO_2 fluxes remains quite large (between 50% and 75%) (Bauer et al., 2013) such that the magnitude and direction of coastal carbon fluxes are not well resolved over annual cycles (Hales et al., 2005). Despite these large uncertainties, it is still believed that coastal ecosystems are responsible for a disproportionately large percentage of global air–sea CO_2 flux, considering the fact that estuaries and continental shelves combined account for less than 10% of ocean surface area (Mackenzie et al., 2005). McLeod et al. (2011) suggested that a critical gap in our understanding of coastal carbon sequestration could be filled by mapping its spatial variability.

There is, therefore, substantial motivation to develop a tool specifically for marine inorganic carbon mapping applications. High resolution upper ocean carbon mapping is valuable in its own right as it has great potential to uncover meaningful biogeochemical patterns that could not be feasibly captured with observation programs limited to bottle sampling (Byrne et al., 2010). Furthermore, such techniques could also be used in a "prospecting" sense—that is, to determine optimal mooring sites prior to long-term static sensor deployments. There have been numerous attempts to characterize the temporal variability of inorganic carbon chemistry using moored autonomous sensors (Frieder et al., 2012; Gray et al., 2012, 2011; Harris et al., 2013; Hofmann et al., 2011; Kapsenberg et al., 2015; Martz et al., 2014, 2009; Price et al., 2012; Yu et al., 2011) and countless spatial surveys of upper ocean carbon dynamics (*e.g.*, Alin et al., 2012; Crosswell et al., 2012; Evans et al., 2013; Evans et al., 2012; Feely et al., 2001; Feely et al., 1998; Manzello et al., 2012; Rérolle et al., 2014; Takahashi et al., 2014; Takahashi et al., 2009; Zhang and Fischer, 2014; Zirino et al., 1986), but few tools exist to continuously

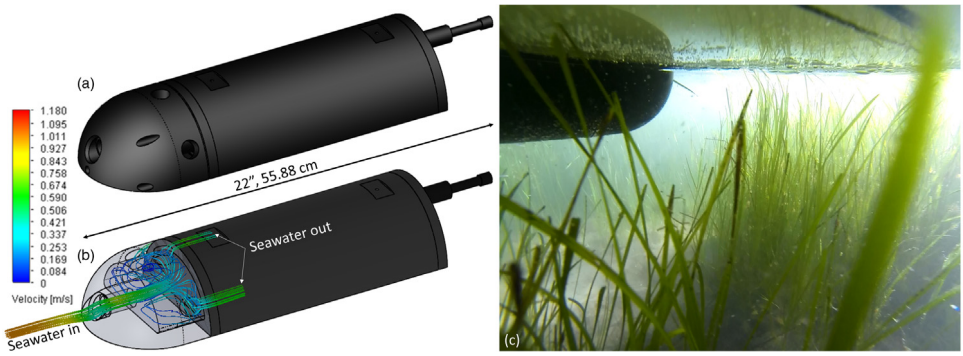

Fig. 1. (a) WavepHOx schematic rendering and (b) flow simulation illustrating streamlines into flow cell inlet and out of the three outlets (two shown, one hidden on opposite side). Flow cell is transparent in (b) to depict the inner cavity where the pH, O_2, and temperature sensing surfaces are located. (c) The WavepHOx deployed on the bottom of a stand-up paddleboard in a shallow eelgrass bed in Mission Bay, CA.

measure near-shore spatial carbon variability. High-quality, autonomous, *in situ* inorganic carbon sensors tend to be bulky, heavy, and not designed for mobile applications. Moreover, there are many fragile ecosystems (*e.g.*, seagrass beds, shallow coral reefs) which larger, motorized vehicles cannot easily access or would likely disturb.

The WavepHOx attempts to overcome this technology gap in order to offer a sensor package for coastal ocean acidification and inorganic carbon mapping studies. The combination of pH and dissolved oxygen provides valuable insight into the mapped area's metabolic state, especially when combined with measurement or estimation of additional CO_2 system variables (*i.e.*, total alkalinity, total dissolved inorganic carbon, or partial pressure of CO_2). It was specifically designed to be incorporated onto low-power and human-powered mobile platforms. To date, the WavepHOx has been deployed primarily on stand-up paddleboards (SUPs), as well as a Liquid Robotics Wave Glider (liquidr.com). These platforms were chosen in order to access shallow, hard-to-reach, and fragile ecosystems, and to deploy the WavepHOx on longer, autonomous expeditions. Similar technology for mobile carbon measurements has been proposed (Willcox et al., 2009) but to our knowledge no sensor data similar to those from WavepHOx have been published. Here we outline design considerations, the WavepHOx configuration, and results from three representative surveys in vegetated ecosystems along the southern California coast.

2. Methods

2.1. Sensor design

The WavepHOx sensor package comprises the ion-selective field effect transistor (ISFET) Honeywell Durafet pH sensor (Martz et al., 2010), Aanderaa oxygen (O_2) optode sensor, and Orion chloride ion selective electrode (Cl-ISE). Both the Durafet and optode include thermistors. The full suite of measured parameters from a WavepHOx includes pH, O_2, and temperature. Details on calculation and quality control of pH data can be found elsewhere (Bresnahan et al., 2014). A custom ARM®-based microcontroller provides data logging and power regulation (from a rechargeable 12 V, 1600 mA h NiMH battery, Tenergy, P/N 11615). All components are enclosed inside a waterproof housing and the Durafet, O_2 optode, and Cl-ISE active sensing surfaces are exposed to seawater but protected by a passively-flushed dome-shaped flow cell (Fig. 1). The sensors were extensively tested and characterized under controlled conditions (temperature, salinity, and pH) in previous work (Bresnahan et al., 2014; Martz et al., 2010; Takeshita et al., 2014).

The flow cell has a single inlet, aligned with the forward direction of the platform, and three outlets, each adjacent to one of the main sensor components. Through the platform's forward movement (nominal speed 0.2–2 knots), water flushes through the flow cell with a residence time of

approximately 2–10 s. Sampling period is user-determined, but can be as fast as 15 s. While sampling at 15 s intervals, the battery nominally lasts 5.4 h for stand-alone applications. Flow simulations were performed using SolidWorks 2014 (with the Flow Simulation add-in) in order to optimize the flow cell's geometry (Fig. 1). The flow cell was designed to flush as rapidly as possible while protecting the sensors from impact and direct sunlight and providing a hydrodynamic cap for the housing.

Electrode conditioning can be a critical limitation when using potentiometric pH sensors, but can be avoided by keeping the components immersed in seawater and never cutting off power to the sensor in between deployments (Bresnahan et al., 2014). The flow cell is filled with seawater or tris buffer in synthetic seawater (DelValls and Dickson, 1998) and inlets/outlets plugged between deployments such that sensor components remain wetted and, therefore, always conditioned to seawater. Additionally, the battery is charged directly through a main bulkhead connector so that power never needs to be cut and recharging can take place without disassembling the housing. The same bulkhead is used for serial communication with the instrument, which is performed both through (1) a direct RS-232 connection between the WavepHOx and a PC or (2) using an AirConsole 2.0 device with the GetConsole iOS application for wireless communication with the WavepHOx and an iPhone/iPad.

2.2. Deployments

We describe results from three WavepHOx deployments—two on a SUP and one on a Wave Glider. While the WavepHOx has two means of measuring pH via the internal and external (*i.e.*, Cl-ISE) reference electrodes (that is, pH^{INT} and pH^{EXT}, respectively), calculation of pH^{EXT} requires salinity which is not presently measured during SUP deployments, but is available from the Sea-Bird Electronics CTD sensor on the Wave Glider. We report pH^{INT} on the total scale here. The sensors used in all deployments were conditioned prior to deployment by operating the assembled WavepHOx in a 6000 L filtered seawater tank at Scripps Institution of Oceanography for two weeks. pH sensor calibration coefficients were determined using spectrophotometric pH (Clayton and Byrne, 1993) of a discrete sample taken from the tank after the sensor's conditioning period (Bresnahan et al., 2014). The optode was calibrated in accordance with the manufacturer's recommendations.

WavepHOx deployments on the SUP utilize an external GPS recorder (Garmin Quatix), synchronized with the sensor's internal clock. The WavepHOx is secured to the bottom of the SUP prior to deployment by pressing it onto 3M Dual Lock Reclosable Fastener (TB3550). Both the WavepHOx housing and SUP have permanently adhered strips of this fastener, allowing for quick assembly and disassembly prior to and after deployments. The sensor is also tethered to an integrated D-ring on the SUP for additional security. Nominal sensor depth during SUP deployments is 10 cm.

The Wave Glider has an internal GPS logger, in addition to several peripheral instruments (*e.g.*, Sea-Bird Electronics CTD, fluorometer, barometric sensors). HDPE clamps fasten the sensor package to the Wave Glider's hull, maintaining the WavepHOx at a nominal depth of 50 cm. The WavepHOx can be powered internally, as described above, or externally by the Wave Glider battery via the main bulkhead connector.

2.2.1. Mission Bay

The WavepHOx was deployed in the Kendall-Frost Mission Bay Marsh Reserve in San Diego, CA (Fig. 2, 32.790°N, 117.227°W) on a SUP from 10:00, 22-Nov-2014, through 09:00, 23-Nov-2014. Sunset was 16:44 on 22-Nov-2014; sunrise the following morning was 06:26 PST. The sampled portion of the reserve has a muddy/sandy bottom with dense eelgrass (*Zostera marina*) patches and is surrounded by a salt marsh. Surveys within a $\sim$300 $\times$ $\sim$200 m grid were repeated roughly every two hours for just under twenty-four consecutive hours. Each survey lasted $\sim$30 min. The WavepHOx sampled at 30 s intervals, slightly below its maximum sampling frequency, in order to conserve power during the 24-hour study. While individual survey durations varied slightly, 782 sensor data points were collected throughout the entire 24-hour study for an average of 55 samples per survey. The sensor was charged once from 00:00 to 03:00, resulting in no sensor data during those hours.

In conjunction with the SUP-mounted WavepHOx, sixty-four discrete seawater samples were collected simultaneously by kayak for total alkalinity (TA) and dissolved inorganic carbon (DIC)

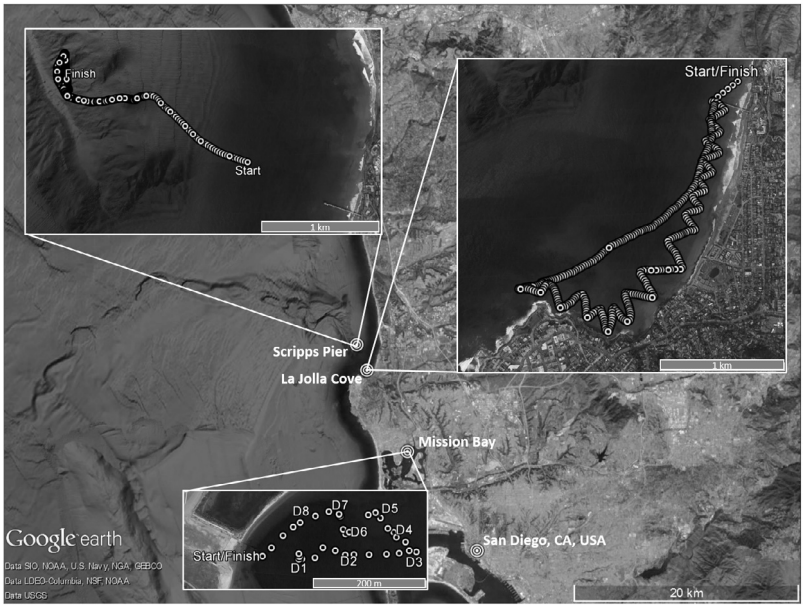

Fig. 2. Map of field sites in San Diego, CA, USA with the survey patterns shown with circular symbols in magnified boxes. The magnified image of the Mission Bay survey also shows the eight locations where discrete samples were collected (D1–D8), eight times each for a total of sixty four discrete samples. Images from Google Earth Pro.

analyses. Samples for TA and DIC were collected in 250 mL Pyrex borosilicate glass bottles and fixed with 100 μL of saturated $HgCl_2$ solution. TA was determined by potentiometric acid titration using 0.1 N HCl standardized against Certified Reference Material (CRM) from Andrew Dickson's laboratory at Scripps Institution of Oceanography. An automated titrator implementing a Metrohm 876 Dosimat Plus dispensing unit and an Ecotrode Plus pH electrode (Metrohm) was used to conduct the titrations. CRMs were run every 5 samples to determine the precision of the system (s.d. $=$ 1.2 μmol kg^{-1}, $n = 20$). DIC was determined using a MARIANDA Automated Infra-Red Inorganic Carbon Analyzer (AIRICA), running CRMs every 3–5 samples to validate system performance (s.d. $=$ 1.2 μmol kg^{-1}, $n = 30$). Temperature (18.7 ± 0.3 °C) and salinity (34.1 ± 0.1) were measured using an Orion 4 Star conductivity probe (Thermo Scientific). pH^{disc} (discrete sample pH on the total scale) was calculated in MATLAB using CO2SYS.m with TA, DIC, temperature, and salinity as inputs (van Heuven et al., 2011).

Sensor pH (pH^{sensor}) was recalibrated to minimize the anomaly between sensor and discrete pH ($n = 56$; the timing of 8 of the 64 discrete samples did not coincide with sensor measurement) (Bresnahan et al., 2014). We also report a Model II least squares fit (Peltzer, 2007) between perturbations in pH^{disc} and pH^{sensor} from the minimum value of pH^{disc}. These perturbation variables, defined as $pH^{disc'} = pH^{disc} - \min(pH^{disc})$ and $pH^{sensor'} = pH^{sensor} - \min(pH^{disc})$, enable careful examination of the Model II fit gain and offset (or slope and y-intercept: c_1 and c_0).

2.2.2. La Jolla Bay

The WavepHOx was also deployed on a SUP in La Jolla Bay, San Diego, CA (Fig. 2, 32.855°N, 117.265°W), on 14-Mar-2015 and 15-Jun-2015. The March study occurred during peak sunlight hours (~14:00) while the June survey was performed on a cloudy morning at sunrise (~06:00), allowing a comparison between photosynthesis-dominated and respiration-dominated patterns, respectively. The bay, largely protected within the Matlahuayl State Marine Reserve, is characterized by variable bottom type: sandy at its northern extent to a mix of rock reef, eelgrass beds (*Zostera marina*), and kelp beds (*e.g.*, *Macrocystis pyrifera*) in the southern portion. Sampling was conducted just offshore of the breaking waves, which were approximately 25 m from shore on average. Significant wave

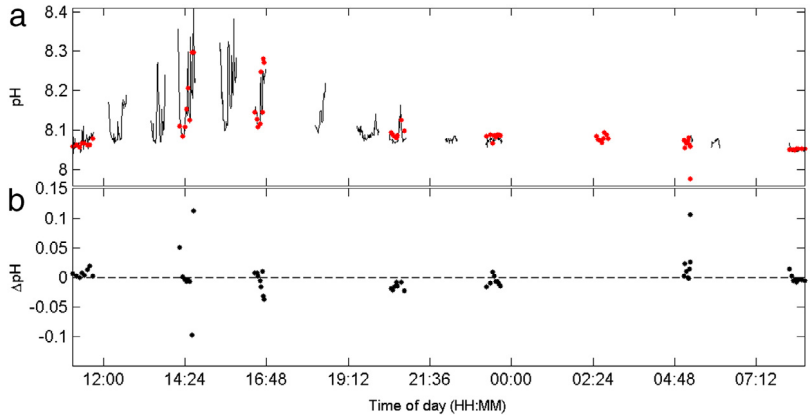

Fig. 3. pH^{sensor} (black line) and $pH^{discrete}$ (red dots) and (b) pH anomaly ($pH^{sensor} - pH^{discrete}$) time-series in the Kendall-Frost Reserve, Mission Bay over 24 h. Note that the sensor was being charged from 00:00 to 03:00. (For interpretation of the references to color in this and following figure legends, the reader is referred to the web version of this article.)

height during the surveys was <60 cm at Scripps Pier (http://cdip.ucsd.edu/), the northernmost extent of the study area, allowing relatively calm conditions for the operator to safely maneuver into very shallow water (<1 m water depth). Salinity, also measured at Scripps pier, was 33.3 (http://www.sccoos.org/data/piers/).

While the only directly measured CO_2 system master variable in this deployment was pH, TA of seawater collected nearby (at the Scripps Pier seawater pump system) has been found to remain within a relatively narrow range of 2200–2250 (TA = 2223 ± 11 μmol kg^{-1} (mean ± s.d.) over three years) (Bockmon et al., 2013). We combine pH_{total} and this average TA in order to calculate DIC, pCO_2, and Ω_{Ar} at *in situ* temperature. pH_{total} and pCO_2 are also calculated at 20 °C (*i.e.*, $pH_{@T=20\ °C}$, $pCO_{2,@T=20\ °C}$) in order to remove the effects of temperature on these parameters. Uncertainties in derived variables resulting from these approximations are discussed. Data analysis was performed with MATLAB R2014b, utilizing the built-in Mapping Toolbox.

2.2.3. Scripps Pier

The final WavepHOx deployment occurred on 19-Dec-2014 on board a Liquid Robotics Wave Glider, just offshore of the La Jolla Bay experiment described above (Fig. 2, 32.876°N, 117.280°W). The Scripps Pier deployment lasted four hours, recorded 959 pH and O_2 measurements, and covered ~4 km cross-shore.

3. Results and discussion

3.1. Mission Bay results

During the Kendall-Frost Reserve 24-hour study, sensor pH varied from 8.04 to 8.41 (range = 0.37) over the 300 m by 200 m grid (Fig. 3(a)). Discrete pH, on the other hand, captured a lower range (range = 0.25 after removal of one statistical outlier during the 05:00 sampling period, defined as >3 standard deviations difference from rest of data in given survey). The majority of variability occurred during daylight hours, due to the photosynthetic activity of the eelgrass. Fig. 3(b) highlights that while sensor and discrete values are in good agreement in general (one standard deviation of the anomaly time-series is 0.028), the largest anomalies tend to occur when natural variability is greatest, reinforcing the difficulty of capturing sensor calibration-quality bottle samples in dynamic environments. Also noteworthy is that while the bottle sampling captures much of the variability and serves as validation for the sensor data, the bottle measurements require significant effort due to laboratory analysis and money due to recurring costs of operating the bench-top systems. For example, measuring DIC and TA on the sixty-four discrete samples required roughly twenty person

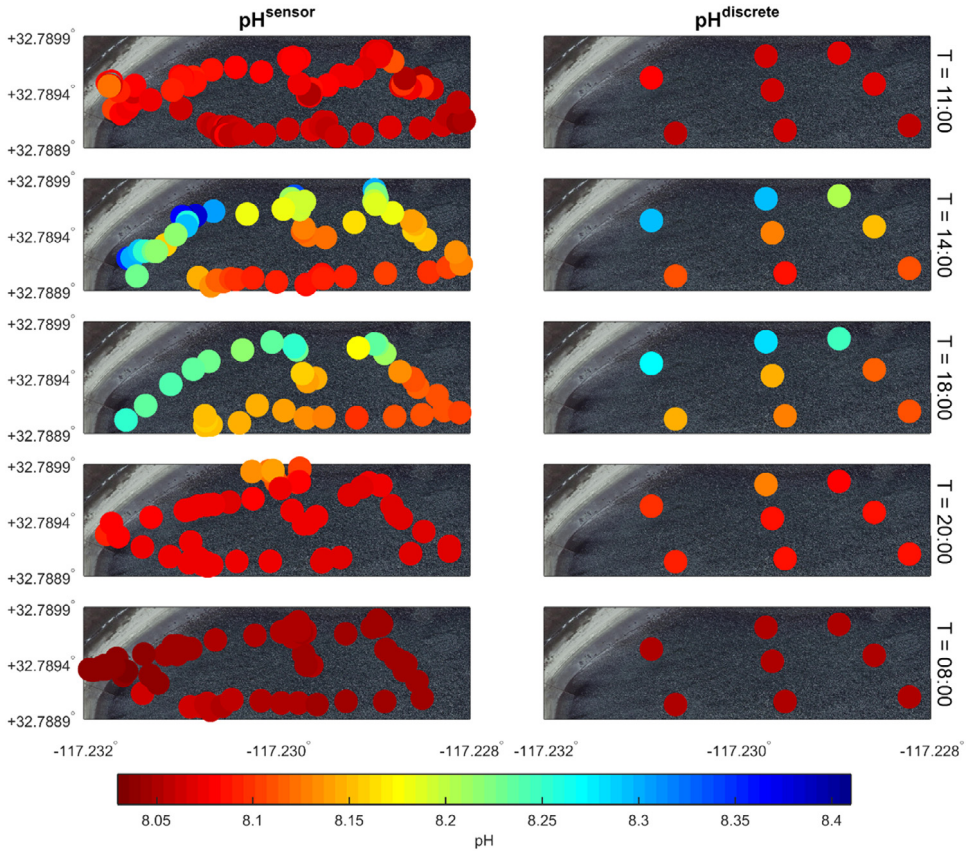

Fig. 4. (Left) Sensor and (right) discrete pH patterns in Mission Bay. Time of each survey is on far right.

hours including typical instrument setup and cleanup procedures. However, bottle samples offer a distinct advantage in that they permit analysis of two marine inorganic carbon system parameters and, therefore, constraint of the CO_2 system.

The features which appear to represent temporal variability when displayed as a time-series (*e.g.*, the afternoon surveys in Fig. 3) are shown to have a very strong spatial component (Fig. 4). In the southeastern extent of the sampled area, characterized by deeper water and lower eelgrass density, pH variability is much lower (pH range < 0.05 over 24 h) while the north-northwestern portion near the salt marsh experiences a large range in pH. It is important to note the similarity between the spatial patterns in pH from the WavepHOx and bottle samples. However, Fig. 4 illustrates the degree of variability lost when using discrete samples alone. Approximately 50% more area was covered using the sensor than using discrete samples, reinforcing the value of an autonomous sensor for biogeochemical mapping.

The property–property plot of $pH^{sensor'}$ vs. $pH^{disc'}$ (Fig. 5) emphasizes the strong agreement between sensor and discrete pH and, importantly, the WavepHOx's ability to track true changes in pH. This finding demonstrates that the flow cell flushes sufficiently quickly relative to (1) the speed of the platform and (2) scales of natural chemical gradients. While a calibration based on a single discrete sample could lead to sensor pH inaccuracy of $\approx$0.1, collecting sixty four samples provides a much better means for quality control. Such a laborious sampling scheme is often unrealistic, but these findings illustrate the WavepHOx's ability to resolve spatiotemporal biogeochemical variability and set a benchmark for the level of accuracy attainable when the sensor is rigorously calibrated and validated. Using similar sensor validation protocols to those described here, the Alliance for Coastal

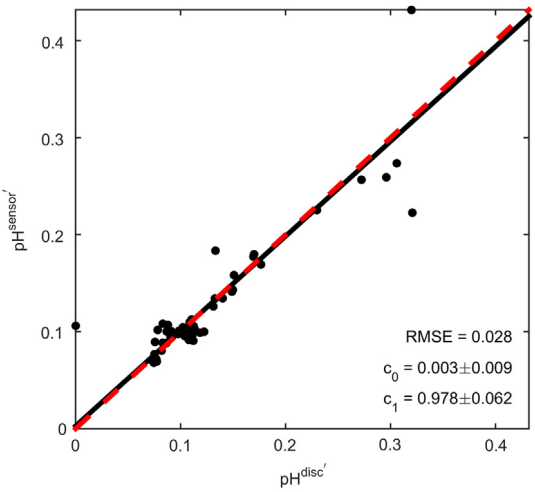

Fig. 5. Property–property plot of $pH^{sensor,}$ vs. $pH^{disc,}$ during Kendall-Frost Reserve twenty-four hour study. The dashed red line represents the 1:1 line ($pH^{sensor,} = pH^{disc,}$) and solid black line is Model II least squares fit (Peltzer, 2007). c_0 and c_1 represent the intercept and slope (alternatively, sensor offset and gain) of the least squares fit. RMSE is the root mean square error.

Technologies (ACT, 2012; http://www.act-us.info/evaluations.php) evaluated seven commercially available pH sensors and reported standard deviations of $pH^{sensor} - pH^{discrete}$ anomaly time-series ranging from ∼0.01–0.1 for at-sea trials. The standard deviation of the pH anomaly time-series shown here (s.d. = 0.028; Fig. 3) and the close fit between pH^{sensor} and $pH^{discrete}$ (Fig. 5), in comparison with the ACT evaluation results, demonstrate the viability of the WavepHOx in oceanographic applications.

3.2. La Jolla Bay SUP results

The two ∼2 h La Jolla Bay deployments (Fig. 6) captured a pH range of 7.75–8.39 and oxygen saturation range from 45.1% to 152.1%. Meanwhile, pCO_2 spiked to over 800 μatm and was drawn down to 145.0 μatm. pH exhibits nearly identical patterns at both *in situ* temperature and at 20 °C, suggesting that the changes seen here are driven by biological processes. Moreover, the spatial patterns suggest that the high pH and oxygen region in the southern, in-shore portion of the survey results from photosynthesis on March 14th (Fig. 7, left); the corresponding low pH and oxygen region on June 15th (Fig. 7, right) results from respiration. The chemical signal from this rarely observed biological hot spot is mixed into the offshore waters, which remain in near equilibrium with the atmosphere at the surface, largely controlling pH (via pCO_2) and O_2.

Measuring a second CO_2 system master variable (*viz.*, TA, DIC, pCO_2) is always recommended (Riebesell et al., 2010) but was not feasible during the La Jolla Bay deployment. A principle design goal for the WavepHOx was to keep the instrument's form factor as small as possible, substantially limiting the number of integral and peripheral instruments that could be incorporated. The low natural historical variability of TA (s.d. = 11 μmol kg^{-1}) (Bockmon et al., 2013) translates to uncertainty in DIC and pCO_2 of approximately 10 μmol kg^{-1} and 2 μatm, respectively. A hypothetical inaccuracy in measured pH of ±0.03 (Bresnahan et al., 2014), for example, would correspond to uncertainty in DIC and pCO_2 of approximately 16 μmol kg^{-1} and 27 μatm, respectively, demonstrating the relative importance of pH sensor calibration compared to knowledge of TA in this ecosystem.

3.3. Scripps Pier results

The Scripps Pier WavepHOx deployment on board the Wave Glider recorded very little variability: pH = 8.048 ± 0.002. As this experiment took place to the northwest of the La Jolla Bay survey depicted in Fig. 7 where little variability was detected, this result is not surprising. The Durafet itself is

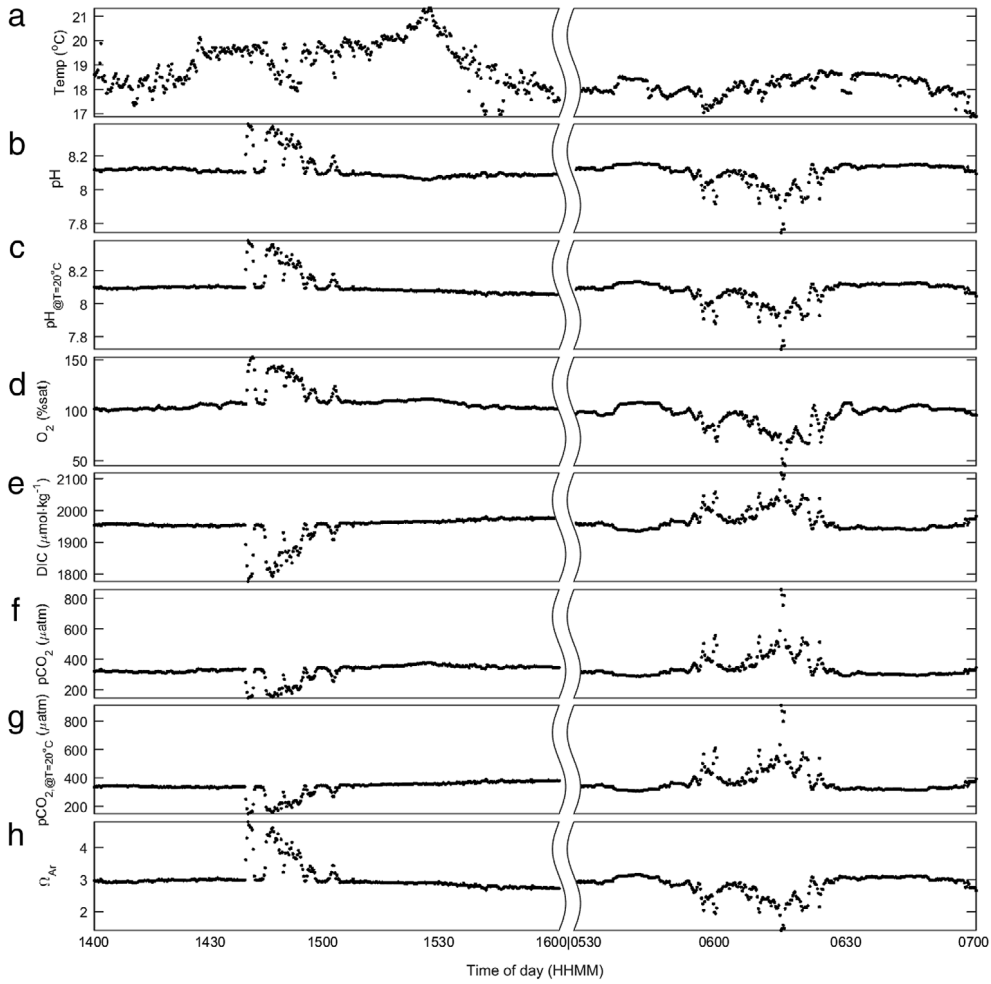

Fig. 6. Time-series of data collected with WavepHOx on (left) 14-Mar-2015 and (right) 15-Jun-2015. Temperature (a), pH (b), and oxygen (d) are measured directly. $pH_{@T=20\ ^\circ C}$ (c), DIC (e), pCO_2 (f), $pCO_{2,@T=20\ ^\circ C}$ (g), and Ω_{Ar} (h) are derived as described in the text. The freely available breakaxis.m function is used to display data from the two surveys on one figure.

stable to 0.0005 pH (Martz et al., 2010), suggesting that any small changes are in fact environmental, not simply instrumental noise, while reinforcing the findings from the La Jolla Bay deployment. We do, however, expect that continued Wave Glider surveys in and beyond this region will uncover interesting spatiotemporal patterns, especially as the survey extent is broadened. The Scripps Pier deployment successfully demonstrated the feasibility of incorporating the WavepHOx into future Wave Glider studies.

3.4. Biogeochemical controls

Photosynthesis and respiration are shown to be primary controls of pH and oxygen variability in the Mission Bay and La Jolla Bay deployments. pH vs. oxygen property–property plots (Supplementary data, Appendix A) demonstrate this tight coupling: in Mission Bay, pH vs. oxygen has a slope of $\partial pH/\partial O_2 = 0.0017$ (O_2 expressed as $\mu mol\ kg^{-1}$) while in La Jolla Bay, the slope is 0.0019. Similar results were found by Frieder et al. (2012) who showed a slope of 0.002 in the nearby La Jolla kelp

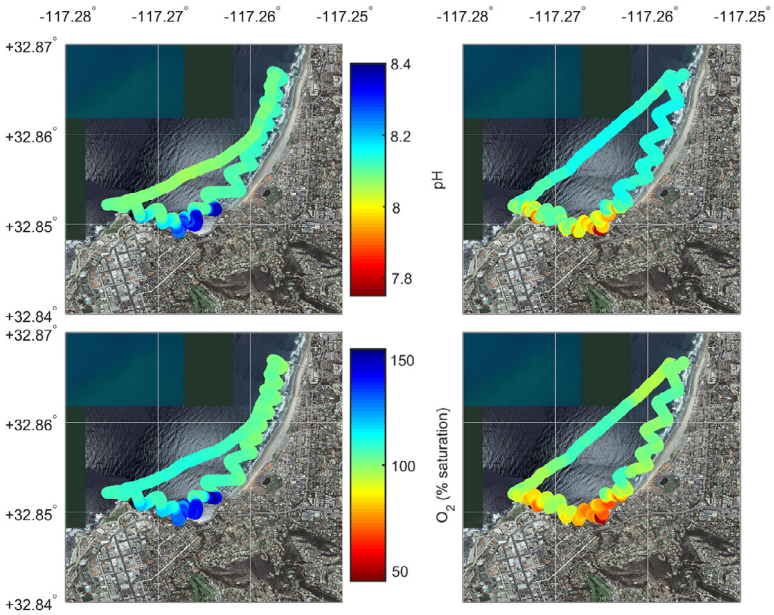

Fig. 7. (Top) pH and (bottom) oxygen patterns in La Jolla Bay on (left) 14-Mar-2015 and (right) 15-Jun-2015.

forest. Similarly, Alin et al. (2012) express pH as a function of temperature and oxygen and show that pH and oxygen co-vary with a slope of 0.00162 at constant temperature. Note that the results of Alin et al. (2012) apply specifically to the California Current System below the mixed layer; the similarity between our results and these previous findings confirms the importance of biological control on the variability we observed. During the Scripps Pier Wave Glider study which took place in the well-ventilated mixed layer and further from biological hotspots, this biologically-mediated relationship breaks down as expected (Supplementary data, Appendix A).

4. Conclusions

We have designed a pH and oxygen sensor package ideal for use on mobile platforms. The WavepHOx shows great promise for high spatiotemporal surface ocean pH and oxygen mapping. Compared with mapping pH with discrete bottle samples, using the WavepHOx is substantially less laborious. Moreover, the sensor is able to capture higher resolution – and sometimes higher magnitude – gradients than a discrete sampling scheme could reasonably achieve. We wish to emphasize that the WavepHOx is not designed specifically for citizen science applications, due to cost (>$10,000) and complexities in sensor care and calibration (Bresnahan et al., 2014). However, supervised deployments by non-experts have been successful, demonstrating that the package can be operated by diverse users within and outside of the professional science community.

At Mission Bay, of the four largest pH anomaly values between sensor and discrete sample (absolute value of ΔpH $>$ 0.05), three occurred during the survey with highest natural variability (14:00, 22-Nov-2014). This finding suggests that neither sensor nor discrete values are necessarily inaccurate, but rather it highlights the difficulties of capturing a discrete sample at the exact same time and place as the instrument. Ecosystems with large spatiotemporal gradients likely require a larger number of discrete samples for sensor calibration and validation. In summary, the utility of bottle samples carried out alongside WavepHOx deployment clearly benefits the resulting dataset by providing validation data, yet the number of bottle samples required to validate an in situ sensor is highly site and user dependent and must be considered on a site-by-site basis (Bresnahan et al., 2014).

The La Jolla Bay deployment shows large changes in inorganic carbon and dissolved oxygen across small spatial scales. Such high spatial variability is often neglected when relying on moored sensors and discrete sampling programs. Continued mapping is necessary to unearth variability across many spatial scales, especially in dynamic coastal waters, and these data must be incorporated in biogeochemical budgets.

The lack of an integrated conductivity/salinity sensor is a notable shortcoming; however, we do not believe it had a significant impact on data quality during these deployments due to small salinity ranges documented in the bottle observations (Mission Bay) and historical records (La Jolla Bay). It could have a larger effect during sampling of ecosystems with large salinity gradients (*e.g.*, estuaries with significant freshwater input). The next version of the WavepHOx will incorporate a miniature conductivity probe.

Lastly, in addition to serving as a powerful oceanographic research tool, the WavepHOx and stand-up paddleboard are a superb science outreach combination, captivating diverse audiences across Southern California. The authors have directly engaged roughly 300 individuals through indoor and outdoor presentations on the science of ocean acidification and the technology used to monitor it. The allure of collecting oceanographic data from stand-up paddleboards is a noteworthy contribution to science outreach approaches.

Acknowledgments

The authors would like to thank Timothy Ray for many inspiring conversations about giving San Diego's youth an opportunity to experience oceanographic fieldwork firsthand. Development and construction of the WavepHOx was funded through an endowment gifted by Andrew Benedek and SUP field deployments were funded through gifts from the Ray family and the Scripps Foundation for Science and the Environment. PJB was supported by the Department of Defense (DoD) through the National Defense Science and Engineering Graduate (NDSEG) Fellowship Program. TW was supported by an NSF-sponsored California Current Ecosystem Long-Term Ecological Research (CCE-LTER) research experience for undergraduates (REU): NSF Award Number 1026607. Ocean Discovery Institute provided the substantial logistical support and supervision necessary to work with middle and high school students throughout this project. Yuichiro Takeshita, Yassir Eddebbar, and Steve Walters were tremendously helpful in offering scientific and outreach guidance throughout the project. Thirty middle and high school students assisted with the Mission Bay deployment with the Ocean Discovery Institute (http://oceandiscoveryinstitute.org/). Students were involved in closely-supervised field sampling, discrete sample analysis, and data analysis.

Appendix A. Supplementary data

Supplementary material related to this article can be found online at http://dx.doi.org/10.1016/j.mio.2016.04.004.

References

ACT, 2012. Alliance for Coastal Technologies: Protocols for the Performance Verification of In Situ pH Sensors.

Alin, S.R., et al., 2012. Robust empirical relationships for estimating the carbonate system in the southern California current system and application to CalCOFI hydrographic cruise data (2005–2011). J. Geophys. Res. 117 (C05033), 1–16. http://dx.doi.org/10.1029/2011jc007511.

Bauer, J.E., et al., 2013. The changing carbon cycle of the coastal ocean. Nature 504 (7478), 61–70. http://dx.doi.org/10.1038/nature12857.

Bockmon, E.E., Frieder, C.A., Navarro, M.O., White-Kershek, L.A., Dickson, A.G., 2013. Technical note: Controlled experimental aquarium system for multi-stressor investigation of carbonate chemistry, oxygen saturation, and temperature. Biogeosciences 10 (9), 5967–5975. http://dx.doi.org/10.5194/bg-10-5967-2013.

Borges, A., 2005. Do we have enough pieces of the jigsaw to integrate CO_2 fluxes in the coastal ocean? Estuaries 28 (1), 3–27. http://dx.doi.org/10.1007/BF02732750.

Borges, A., et al. 2010. A global sea surface carbon observing system: Inorganic and organic carbon dynamics in coastal oceans. In: J. Hall, D.E. Harrison and D. Stammer (Editors), Proceedings of OceanObs'09: Sustained Ocean Observations and Information for Society, Vol. 2, Venice Italy. http://dx.doi.org/10.5270/OceanObs09.cwp.07.

Borges, A.V., Schiettecatte, L.S., Abril, G., Delille, B., Gazeau, F., 2006. Carbon dioxide in European coastal waters. Estuar. Coast. Shelf Sci. 70 (3), 375–387. http://dx.doi.org/10.1016/j.ecss.2006.05.046.

Bresnahan, P.J., Martz, T.R., Takeshita, Y., Johnson, K.S., LaShomb, M., 2014. Best practices for autonomous measurement of seawater pH with the Honeywell Durafet. Methods Oceanogr. 9, 44–60. http://dx.doi.org/10.1016/j.mio.2014.08.003.

Byrne, R.H., et al., 2010. Sensors and systems for in situ observations of marine carbon dioxide system variables. In: Proceedings of OceanObs'09: Sustained Ocean Observations and Information for Society, Vol. 2. ESA Publication WPP-306, Venice, Italy, http://dx.doi.org/10.5270/OceanObs09.cwp.13.

Cai, W.J., 2011. Estuarine and coastal ocean carbon paradox: CO_2 sinks or sites of terrestrial carbon incineration? Annu. Rev. Mar. Sci. 3, 123–145. http://dx.doi.org/10.1146/annurev-marine-120709-142723.

Chen, C.-T.A., Borges, A.V., 2009. Reconciling opposing views on carbon cycling in the coastal ocean: Continental shelves as sinks and near-shore ecosystems as sources of atmospheric CO_2. Deep Sea Res. Part II 56 (8–10), 578–590. http://dx.doi.org/10.1016/j.dsr2.2009.01.001.

Clayton, T.D., Byrne, R.H., 1993. Spectrophotometric seawater pH measurements: total hydrogen ion concentration scale calibration of m-cresol purple and at-sea results. Deep-Sea Res. I 40 (10), 2115–2129. http://dx.doi.org/10.1016/0967-0637(93)90048-8.

Crosswell, J.R., Wetz, M.S., Hales, B., Paerl, H.W., 2012. Air–water CO_2 fluxes in the microtidal Neuse River Estuary, North Carolina. J. Geophys. Res. 117 (C08017), 1–12. http://dx.doi.org/10.1029/2012jc007925.

DelValls, T.A., Dickson, A.G., 1998. The pH of buffers based on 2-amino-2-hydroxymethyl-1,3-propanediol ('tris') in synthetic sea water. Deep-Sea Res. I 45 (9), 1541–1554. http://dx.doi.org/10.1016/S0967-0637(98)00019-3.

Evans, W., Hales, B., Strutton, P.G., 2013. pCO_2 distributions and air–water CO_2 fluxes in the Columbia River estuary. Estuar. Coast. Shelf Sci. 117, 260–272. http://dx.doi.org/10.1016/j.ecss.2012.12.003.

Evans, W., Hales, B., Strutton, P.G., Ianson, D., 2012. Sea–air CO_2 fluxes in the western Canadian coastal ocean. Prog. Oceanogr. 101 (1), 78–91. http://dx.doi.org/10.1016/j.pocean.2012.01.003.

Feely, R.A., et al., 1998. A new automated underway system for making high precision pCO_2 measurements onboard research ships. Anal. Chim. Acta 377, 185–191. http://dx.doi.org/10.1016/S0003-2670(98)00388-2.

Feely, R., Sabine, C., Takahashi, T., Wanninkhof, R., 2001. Uptake and storage of carbon dioxide in the ocean: The global CO_2 survey. Oceanography 14 (4), 18–32. http://dx.doi.org/10.5670/oceanog.2001.03.

Frieder, C.A., Nam, S.H., Martz, T.R., Levin, L.A., 2012. High temporal and spatial variability of dissolved oxygen and pH in a nearshore California kelp forest. Biogeosciences 9 (10), 3917–3930. http://dx.doi.org/10.5194/bg-9-3917-2012.

Gattuso, J.P., Frankignoulle, M., Wollast, R., 1998. Carbon and carbonate metabolism in coastal aquatic ecosystems. Annu. Rev. Ecol. Syst. 29 (1), 405–434. http://dx.doi.org/10.1146/annurev.ecolsys.29.1.405.

Gray, S.E.C., et al., 2011. Applications of in situ pH measurements for inorganic carbon calculations. Mar. Chem. 125, 82–90. http://dx.doi.org/10.1016/j.marchem.2011.02.005.

Gray, S.E.C., DeGrandpre, M.D., Langdon, C., Corredor, J.E., 2012. Short-term and seasonal pH, pCO_2 and saturation state variability in a coral-reef ecosystem. Glob. Biogeochem. Cycles 26 (GB3012), 1–13. http://dx.doi.org/10.1029/2011gb004114.

Hales, B., Takahashi, T., Bandstra, L., 2005. Atmospheric CO_2 uptake by a coastal upwelling system. Glob. Biogeochem. Cycles 19 (GB1009), 1–11. http://dx.doi.org/10.1029/2004GB002295.

Harris, K.E., DeGrandpre, M.D., Hales, B., 2013. Aragonite saturation state dynamics in a coastal upwelling zone. Geophys. Res. Lett. 40 (11), 2720–2725. http://dx.doi.org/10.1002/grl.50460.

Hofmann, G.E., et al., 2011. High-frequency dynamics of ocean pH: a multi-ecosystem comparison. PLoS One 6 (12), e28983. http://dx.doi.org/10.1371/journal.pone.0028983.

Kapsenberg, L., Kelley, A.L., Shaw, E.C., Martz, T.R., Hofmann, G.E., 2015. Near-shore Antarctic pH variability has implications for the design of ocean acidification experiments. Sci. Rep. 5, http://dx.doi.org/10.1038/srep09638.

Laruelle, G.G., Dürr, H.H., Slomp, C.P., Borges, A.V., 2010. Evaluation of sinks and sources of CO_2 in the global coastal ocean using a spatially-explicit typology of estuaries and continental shelves. Geophys. Res. Lett. 37 (15), L15607. http://dx.doi.org/10.1029/2010GL043691.

Mackenzie, F.T., Andersson, A., Lerman, A., Ver, L.M., 2005. Boundary exchanges in the global coastal margin: implications for the organic and inorganic carbon cycles. In: Robinson, A.R., Brink, K.H. (Eds.), The Sea: Ideas and Observations on Progress in the Study of Seas. The President and Fellows of Harvard College, USA, pp. 193–225.

Manzello, D.P., Enochs, I.C., Melo, N., Gledhill, D.K., Johns, E.M., 2012. Ocean acidification refugia of the Florida reef tract. PLoS One 7 (7), e41715. http://dx.doi.org/10.1371/journal.pone.0041715.

Martz, T., et al., 2014. Dynamic variability of biogeochemical ratios in the Southern California current system. Geophys. Res. Lett. 41 (7), 2496–2501. http://dx.doi.org/10.1002/2014gl059332.

Martz, T.R., Connery, J.G., Johnson, K.S., 2010. Testing the Honeywell Durafet for seawater pH applications. Limnol. Oceanogr.: Methods 8, 172–184. http://dx.doi.org/10.4319/lom.2010.8.172.

Martz, T.R., DeGrandpre, M.D., Strutton, P.G., McGillis, W.R., Drennan, W.M., 2009. Sea surface pCO_2 and carbon export during the Labrador Sea spring-summer bloom: An in situ mass balance approach. J. Geophys. Res. 114 (C09008), 1–12. http://dx.doi.org/10.1029/2008jc005060.

McLeod, E., et al., 2011. A blueprint for blue carbon: toward an improved understanding of the role of vegetated coastal habitats in sequestering CO_2. Front. Ecol. Environ. 9 (10), 552–560. http://dx.doi.org/10.1890/110004.

Peltzer, E., 2007. Model II least squares fit: lsqfitma.m. http://www.mbari.org/staff/etp3/regress/lsqfitma.m.

Price, N.N., Martz, T.R., Brainard, R.E., Smith, J.E., 2012. Diel variability in seawater pH relates to calcification and benthic community structure on coral reefs. PLoS One 7 (8), e43843. http://dx.doi.org/10.1371/journal.pone.0043843.

Rérolle, V.M.C., et al., 2014. Controls on pH in surface waters of northwestern European shelf seas. Biogeosci. Discuss. 11 (1), 943–974. http://dx.doi.org/10.5194/bgd-11-943-2014.

Riebesell, U., Fabry, V., Hansson, L., Gattuso, J.-P. (Eds.), 2010. Guide to Best Practices for Ocean Acidification Research and Data Reporting. p. 260.

Takahashi, T., et al., 2009. Climatological mean and decadal change in surface ocean pCO_2, and net sea–air CO_2 flux over the global oceans. Deep Sea Res. Part II 56 (8–10), 554–577. http://dx.doi.org/10.1016/j.dsr2.2008.12.009.

Takahashi, T., et al., 2014. Climatological distributions of pH, pCO_2, total CO_2, alkalinity, and CaCO3 saturation in the global surface ocean, and temporal changes at selected locations. Mar. Chem. 164, 95–125. http://dx.doi.org/10.1016/j.marchem.2014.06.004.

Takeshita, Y., Martz, T.R., Johnson, K.S., Dickson, A.G., 2014. Characterization of an ion sensitive field effect transistor and chloride ion selective electrodes for pH measurements in seawater. Anal. Chem. 86 (22), 11189–11195. http://dx.doi.org/10.1021/ac502631z.

van Heuven, S., Pierrot, D., Rae, J.W.B., Lewis, E., Wallace, D.W.R., 2011. MATLAB Program Developed for CO_2 System Calculations. ORNL/CDIAC-105b. Carbon Dioxide Information Analysis Center. Oak Ridge National Laboratory. US Department of Energy, Oak Ridge, Tennessee. http://dx.doi.org/10.3334/CDIAC/otg.CO2SYS_MATLAB_v1.1.

Willcox, S., et al. 2009. An autonomous mobile platform for underway surface carbon measurements in open-ocean and coastal waters. In: OCEANS 2009, MTS/IEEE Biloxi—Marine Technology for Our Future: Global and Local Challenges, pp. 1–8.

Yu, P.C., Matson, P.G., Martz, T.R., Hofmann, G.E., 2011. The ocean acidification seascape and its relationship to the performance of calcifying marine invertebrates: Laboratory experiments on the development of urchin larvae framed by environmentally-relevant pCO_2/pH. J. Exp. Mar. Biol. Ecol. 400 (1–2), 288–295. http://dx.doi.org/10.1016/j.jembe.2011.02.016.

Zhang, J.Z., Fischer, C.J., 2014. Carbon dynamics of Florida Bay: spatiotemporal patterns and biological control. Environ. Sci. Technol. 48 (16), 9161–9169. http://dx.doi.org/10.1021/es500510z.

Zirino, A., et al., 1986. pH-temperature–nutrient relationships in the eastern tropical Pacific Ocean. Sci. Total Environ. 58 (1–2), 117–137. http://dx.doi.org/10.1016/0048-9697(86)90082-3.